Mater. Res. Soc. Symp. Proc. Vol. 892 © 2006 Materials Research Society 0892-FF18-09-EE09-09.1

Characteristics of a phosphorus-doped *p*-type ZnO film by MBE

F. X. Xiu, Z. Yang, L. J. Mandalapu, and J. L. Liu
Department of Electrical Engineering, Quantum Structures Laboratory,
University of California, Riverside, CA 92521, U.S.A.

ABSTRACT

A solid-source GaP effusion cell was used to provide phosphorus dopants to achieve *p*-type ZnO with molecular-beam epitaxy (MBE). Room temperature (RT) Hall-effect measurements reveal that phosphorus-doped ZnO has a strong *p*-type conduction with a hole concentration of 6.5×10^{18} cm^{-3} and a hole mobility of 9.0 cm^2/V s. X-ray diffraction measurements show a preferential growth orientation along <11-20> by θ-2θ scan and a tilt of ZnO (11-20) plane relative to the substrate surface by rocking curve and reciprocal space map. Photoluminescence (PL) spectra at 8.5 K show a dominant acceptor-bound exciton emission at 3.319 eV. The acceptor energy level of the phosphorus dopant is calculated to be 0.18 eV above the valence band from PL spectra, which is consistent with the temperature dependence of PL measurements.

INTRODUCTION

With substantial research interest, ZnO has been recognized as a promising material for blue/ultraviolet optoelectronics, spintronics, high temperature electronics and transparent electronics. However, *p*-type ZnO is difficult to fabricate because of lack of suitable *p*-dopants to make it reliable and reproducible. This difficulty has restrained the progress of ZnO applications to a great extent.

In recent years, tremendous efforts have been made towards *p*-type ZnO with different dopants via many growth techniques. Candidates are mainly group V elements, such as nitrogen [1,2], phosphorous [3-5], arsenic [6,7], and antimony [8,9]. Among them, phosphorus-doped ZnO films were demonstrated to have good electrical properties, such as high carrier concentration, reasonable mobility, low resistivity, etc [3,5]. However, nowadays phosphorus-doped ZnO films are mainly fabricated by pulsed laser deposition [4] and radio-frequency sputtering methods [5]. Unlike MBE technique, high-quality single crystalline ZnO films are difficult to obtain. In addition, the dopant source, for example P_2O_5, must be thermally dissociated to provide the phosphorus dopants after growth. Unfortunately, this process largely depends on rapid thermal annealing conditions and may yield irreproducible *p*-type conduction. Finally, some phosphorus-based compounds that are currently being used, such as Zn_3P_2, are toxic in nature. Therefore, a better dopant source along with a good growth technique is highly desirable.

In this study, a solid-source GaP effusion cell was used to provide phosphorus dopants in an SVTA MBE system. A detailed description of special features of GaP effusion cell was reported elsewhere [10]. The special design ensures the generation of a Ga-free P_2 beam upon heating up the GaP effusion cell at high temperatures. The simple operation of GaP effusion

cell and good controllability of P_2 beam make this doping technique an advantageous alternative for ZnO *p*-type phosphorus doping.

EXPERIMENTAL DETAILS

Undoped and phosphorus-doped ZnO films were grown on (01-12) r-plane sapphire substrates. Detailed growth procedures can be found elsewhere [10]. The key factor is that an oxygen-rich condition was adopted to minimize the formation of zinc interstitials and oxygen vacancies. After growth, *in situ* annealing was performed at 800 ˚C for 20 min under vacuum to activate the phosphorus dopants. Electrical properties, structural properties and optical properties were comprehensively investigated to study the phosphorus doping effect.

DISCUSSION

Electrical properties

A home-built Hall-effect measurement system equipped with a 3500 G magnet was utilized for RT measurements. The undoped and phosphorus-doped ZnO films were cut into 5 mm×5 mm pieces; metal contacts were subsequently deposited on top in the van der Pauw configuration by an *e*-beam evaporator. The metal scheme consists of Ti and Al layers with the thickness of 10 and 400 nm, respectively. Linear characterizations of current-voltage curves were observed, indicating the formation of good-quality Ohmic contacts on both *n*-type and *p*-type ZnO films.

RT electrical properties of the undoped and phosphorus-doped ZnO films are shown in Table I. The undoped sample shows an *n*-type conductivity with a carrier concentration of 1.0×10^{17} cm^{-3} and a mobility of 46.5 cm^2/V s. The origin of *n*-type conduction is widely believed to arise from the contributions of zinc interstitials and/or hydrogen impurities, which serve as shallow donors to provide electrons [11,12].The phosphorus-doped ZnO, however, shows strong *p*-type conduction with a hole concentration of 6.5×10^{18} cm^{-3} and a hole mobility of 9.0 cm^2/V s. Temperature dependence of hole concentration further confirmed the *p*-type conduction by phosphorus doping [10].Although the doping mechanism remains unclear and under debate, the successful demonstration of *p*-type ZnO in our experiments indicates that GaP can be an alternative phosphorus dopant source to realize *p*-type layers with good electrical properties.

Structural properties

In our previous study, x-ray θ-2θ scans were performed to investigate ZnO growth orientations. It was found that ZnO has a preferential growth direction along <11-20> on r-plane sapphire. Based on this result, it can be inferred that the *c*-axis lies in the surface plane (11-20) of ZnO film. This orientation indeed offers an advantage. The lattice mismatch along the *c*-axis is 1.53%, while the mismatch along the direction perpendicular to the *c*-axis

is 18.3%. Therefore, the overall lattice mismatch is less than that of (0001) ZnO on *c*-plane sapphire [13].

TABLE I. RT electrical properties of undoped and phosphorus-doped ZnO films.

Sample	GaP cell temp. (˚C)	Type	Thickness (μm)	Mobility (cm^2/V s)	Carrier density (cm^{-3})
Undoped	N/A	*n*	0.5	46.5	1.0×10^{17}
Phosphorus-doped	750	*p*	0.5	9.0	6.5×10^{18}

X-ray rocking scans (ω) were also performed to further study the structural properties of undoped and phosphorus-doped ZnO. The spectra on the (11-20) plane are given in figure 1 along with their fitted results. The full width at half maximum (FWHM) values of 0.35°and 0.47° are obtained for undoped and phosphorus-doped films, respectively. It is well known that Δ ω reflects the broadening due to microscopic tilts of the plane [14]. Therefore, phosphorus incorporation during growth induces the tilt of the (11-20) plane. This result is in a good agreement with our previous RHEED observations, which showed a three-dimensional growth mode for the phosphorus-doped film [10].

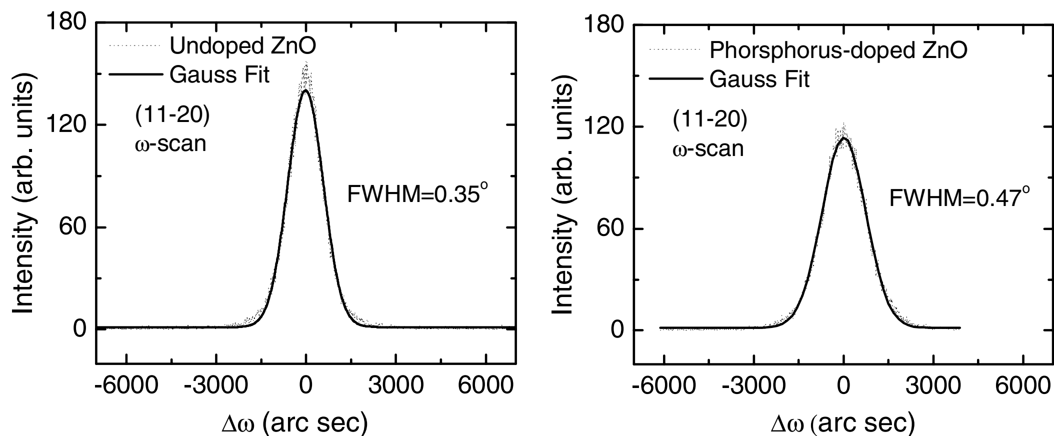

Figure 1. Rocking curves for undoped ZnO and phosphorus-doped ZnO. The measured (dot) results were fitted (solid) to obtain FWHM values by Gauss fit.

The mosaic structure of phosphorus-doped ZnO, as discussed above, is clearly shown in figure 2, where a reciprocal space map is taken around the (02-24) sapphire substrate and (11-20) ZnO. Mosaicity results in the elongation of the ZnO peak along the Δq_x direction. A remarkable feature of the ZnO layer is that it is tilted with respect to the substrate, as can be deduced from the fact that the peaks corresponding to the film and to the substrate are not aligned along the Δq_z direction.

Optical properties

Low temperature (LT) PL measurements were carried out to investigate the optical

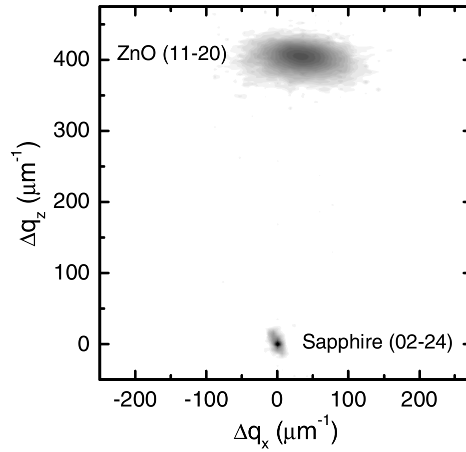

Figure 2. A reciprocal space map around the (02-24) Bragg reflection of a sapphire substrate.

properties of undoped and phosphorus-doped ZnO films with a 325 nm He–Cd laser operated with a power of 5 mW. Figure 3(a) shows a spectrum for the undoped ZnO film measured at 8.5 K. A near-band-edge emission associated with the neutral-donor-bound exciton ($D^o X$) is observed at 3.366 eV, which is attributed to native defects (Zn_i) [11] and/or incorporated hydrogen impurities [12]. For the phosphorus-doped ZnO, the emissions at 3.360, 3.319, 3.253 and 3.181 eV were identified as $D^o X$, $A^o X$ (neutral-acceptor-bound exciton), FA (free electron to acceptor level), and DAP (donor-acceptor pair) transitions, respectively [10]. It is also found that, similar to phosphorus-doped ZnO, the undoped film shows emissions at 3.317, 3.259 and 3.177 eV, which might arise from a small incorporation of residual phosphorus inside the chamber during the film growth.

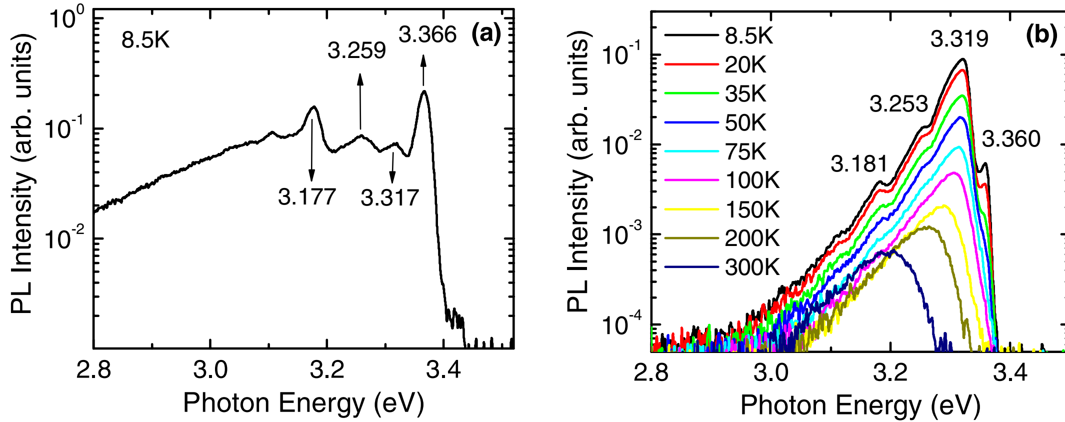

Figure 3. LT PL spectra for (a) undoped ZnO at 8.5 K (b) phosphorus-doped ZnO at temperatures ranging from 8.5 to 300 K.

The binding energy of a phosphorus acceptor E_A can be calculated with the formula [6]

$$E_A = E_{gap} - E_{FA} + k_B T / 2 \, . \tag{1}$$

With an intrinsic band gap of E_{gap} = 3.437 eV [3,6], the value of E_A is obtained as 0.18 eV. To further confirm the acceptor binding energy, temperature dependence of PL measurements was performed on the phosphorus-doped ZnO film at temperatures ranging from 8.5 to 300 K,

as shown in figure 3(b).

In conjunction with temperature-dependent PL spectra, the energy-integrated intensity of the $A^{o}X$ emission is shown as a function of temperature in figure 4. The luminescence intensity quenches exponentially in the temperature region from 8.5 to 150 K. The temperature dependence of the integrated PL intensity is given by [7]

$$I(T) = I_0 / [1 + C\exp(-E_b^{A^o X} / kT)], \tag{2}$$

where C is a fitting parameter, I_o is the integrated PL intensity at $T = 0$ K, which is approximately the same as at $T = 8$ K, and $E_b^{A^o X}$ is the binding energy between the acceptor and free exciton. From the fitting, $E_b^{A^o X} = 17.0\,\text{meV}$ was obtained. Applying the Haynes rule $E_b^{A^o X} / E_A \approx 0.1$ to ZnO material system [6,7], an acceptor activation energy E_A is estimated to be 170 meV. This result is consistent with the value for the acceptor binding energy of 0.18 eV obtained from Eq. (1).

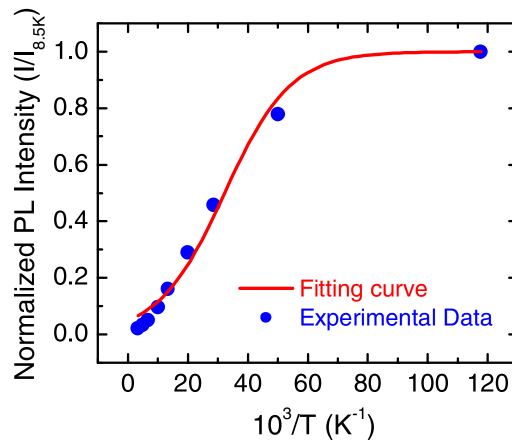

Figure 4. Integrated intensity of the $A^{o}X$ emission as a function of temperature. The dots represent the experimental data, and the solid line is the fit to Eq. (2).

CONCLUSIONS

In summary, a phosphorus-doped *p*-type ZnO film was realized by using a GaP effusion cell as a phosphorus dopant source in a MBE system. Hall-effect measurements reveal that the phosphorus-doped ZnO film has a *p*-type conduction. A hole concentration of 6.5×10^{18} cm^{-3} and a hole Hall mobility of 9.0 cm^2/V s were measured in this film. Structural properties show that both undoped and phosphorus doped ZnO films grown on r-plane sapphire show a preferential growth orientation along <11-20>. The rocking curve and reciprocal space map demonstrate that the ZnO (11-20) plane is tilted relative to the substrate surface, especially for the phosphorus-doped film. The LT PL spectra show a strong peak at 3.319 eV, attributing

to the phosphorus-associated $A^o X$ emission. From these data, the activation energy of phosphorus is estimated to be 0.18 eV, which is in a good agreement with the temperature dependence of PL spectra.

ACKNOWLEDGMENTS

This work was supported by DARPA/DMEA through the center for NanoScience and Innovation for Defense (CNID) under the award No. H94003-04-2-0404. The authors would like to acknowledge Mr. Joo-Young Lee (Electrical Engineering Department at UCLA) for RT Hall-effect measurements and Mr. Atif M. Noori (Materials Science Department at UCLA) for x-ray diffraction measurements.

REFERENCES

1. A. Tsukazaki, A. Ohtomo, T. Onuma, M. Ohtani, T. Makino, M. Sumiya, K. Ohtani, S. F. Chichibu, S. Fuke, Y. Segawa, H. Ohno, H. Koinuma, and M. Kawasaki, Nat. Mater. **4**, 42 (2005).
2. D. C. Look, D. C. Reynolds, C. W. Litton, R. L. Jones, D. B. Eason, and G. Cantwell, Appl. Phys. Lett. **81**, 1830 (2002).
3. D. K. Hwang, H. S. Kim, J. H. Lim, J. Y. Oh, J. H. Yang, S. J. Park, K. K. Kim, D. C. Look, and Y. S. Park, Appl. Phys. Lett. **86**, 151917 (2005).
4. V. Vaithianathan, B. T. Lee, and S. S. Kim, Phys. Status Solidi A **201**, 2837 (2004).
5. K. K. Kim, H. S. Kim, D. K. Hwang, J. H. Lim, and S. J. Park, Appl. Phys. Lett. **83**, 63 (2003).
6. Y. R. Ryu, T. S. Lee, and H. W. White, Appl. Phys. Lett. **83**, 87 (2003).
7. T. S. Jeong, M. S. Han, C. J. Youn, and Y. S. Park, J. Appl. Phys. **96**, 175 (2004).
8. F. X. Xiu, Z. Yang, L. J. Mandalapu, D. T. Zhao, J. L. Liu, and W. P. Beyermann, Appl. Phys. Lett. **87**, 152101 (2005).
9. F. X. Xiu, Z. Yang, L. J. Mandalapu, D. T. Zhao, and J. L. Liu, Appl. Phys. Lett. (In press).
10. F. X. Xiu, Z. Yang, L. J. Mandalapu, J. L. Liu, and W. P. Beyermann, Appl. Phys. Lett. (In press).
11. S. B. Zhang, S. H. Wei, and A. Zunger, Phys. Rev. B **63**, 075205 (2001).
12. C. G. Van de Walle, Phys. Rev. Lett. **85**, 1012 (2000).
13. H. Sheng, S. Muthukumar, N. W. Emanetoglu, and Y. Lu, Appl. Phys. Lett. **80**, 2132 (2002).
14. J. Zuniga-Perez, C. Munuera, C. Ocal, V. Munoz-Sanjose, J. Cryst. Growth, **271**, 223 (2004).